Low Power Adaptive Power Management with Energy Aware Interface for Wireless Sensor Nodes Powered Using Piezoelectric Energy Harvesting

Zheng Jun Chew and Meiling Zhu
College of Engineering, Mathematics and Physical Sciences,
University of Exeter,
Exeter EX4 4QF UK
z.j.chew@exeter.ac.uk, m.zhu@exeter.ac.uk

***Abstract*—A batteryless power management circuit incorporating an energy aware interface (EAI) for wireless sensor nodes (WSNs) powered by piezoelectric energy harvester (PEH) has been proposed and implemented. Traditional power management usually requires two DC–DC converters, each for maximum power point tracking (MPPT) and voltage regulation functionalities. The proposed circuit requires only one DC-DC converter for both the MPPT and voltage regulation. The EAI also provides a means to voltage regulation. This allows the circuit to have higher efficiency as the energy transfer does not have to go through two stages to reach the load. A PEH connected to the proposed circuit was tested under various vibration conditions. The circuit was found to have end-to-end efficiency of about 66% under most of the test conditions.**

Keywords— Energy harvesting, Energy storage, Piezoelectric energy harvester, Power management

I. INTRODUCTION

Technology advancements in semiconductor industries over the years see the emergence of many low power electronic devices such as wireless sensors which consume milliwatts of power or less [1]. Therefore, it is viable to power these devices using energy such as vibration, solar and temperature from the ambient environment with proper energy management since energy harvesters of these sources have a power density of more than 100μW/cm^3 [2]. The use of energy harvesting technologies can essentially eliminate batteries from the WSNs. Vibration can be harvested almost anytime and anywhere directly by a transducer as vibration can occur either naturally from the environment or induced by means of other sources. This made vibration-based energy harvesting particular attractive and gained a lot of research interests.

PEH is one of the most popular transducers used to scavenge vibration energy due to its simplicity, rigidity and attractive power generation capability [1-3]. A common power management module is shown in Fig. 1 [4, 5]. This approach requires two DC–DC converters in series. Microcontroller is used to perform maximum power point tracking (MPPT) algorithm to achieve resistance matching with the energy harvester by actively varying the duty cycle of the first DC–DC converter. The harvested energy will be stored in the storage capacitor. The variation in duty cycle of a DC–DC converter resulted in an output voltage which is not constant. The second DC–DC converter will regulate the voltage across the storage capacitor to a stable voltage level suitable for the electronics devices. The use of two DC–DC converters makes the overall system bulky and less efficient as the energy has to go through more conversion stages.

This work herein demonstrates a power management circuit for PEHs which incorporates only one DC–DC converter. The circuit was constructed entirely out of commercially available components, making it simple and low cost to build. This circuit is used to manage the energy flow of a PEH subjected to various loadings and frequencies to show the adaptability of the proposed design under different vibrating conditions. It was found that the circuit improves the amount of extracted power from a PEH independent of its frequency and strain level experienced. Overall efficiency of the prototyped circuit reaches 66% under most test conditions.

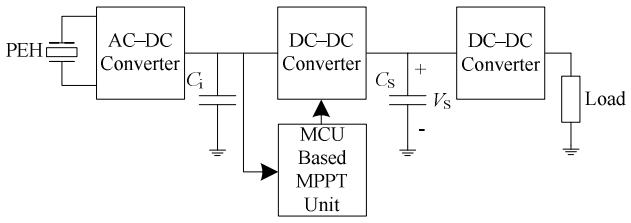

Fig. 1. Conventional two-stage power management circuit for batteryless system.

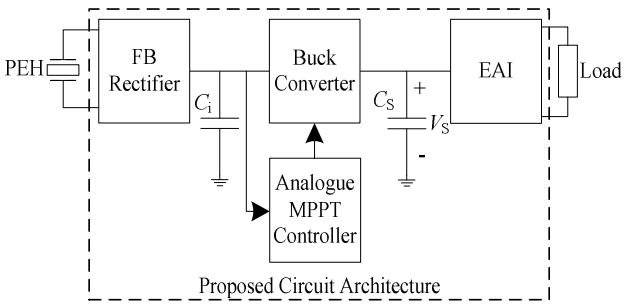

Fig. 2. Proposed batteryless power management circuit.

This work was partially supported by Innovate UK (TSB 29640-211185) and EPSRC (EP/K017950/1).

978-1-4799-8203-5/15/$31.00 ©2015 IEEE

II. SYSTEM ARCHITECTURE

A. Circuit Implementation

The proposed power management circuit has four main subsystems, namely full-wave bridge (FB) rectifier, buck converter, analogue MPPT controller, and energy aware interface (EAI) as shown in Fig. 2. The controller of buck converter used is a commercially available integrated circuit (IC) [6]. Therefore, the other subsystems where simply added onto this IC. Schottky diodes with low reverse current are used to build the FB rectifier to ensure low loss at the rectifier. C_i is the input capacitor to smooth out the rectified voltage from the PEH and also acting as an intermediate storage. The main storage capacitor C_S is a supercapacitor because this type of capacitor has the highest energy density among all types of capacitors, making it a good substitute to battery. Buck converter is chosen because the PEH produces voltage which is usually higher than that a wireless sensor node required. The storage capacitor can also be safely charged directly by the buck converter since supercapacitor usually has a low voltage rating. The EAI will only allow C_S to discharge through the WSN when the voltage level V_S across C_S reaches a preset threshold voltage and stop the energy transfer when V_S drops below another threshold voltage [7]. C_S will then be able to recharge back to the required voltage level for energy release. Therefore, this interface can also act as a voltage regulator to both the electronics load and the storage capacitor, ensuring that V_S does not exceed the voltage limit of those devices. Parameters of these components are summarized in Table I.

B. Circuit Operation

Electrical energy from the PEH is rectified by the FB rectifier and stored in C_i. The analogue MPPT controller will determine the maximum power point (MPP) of the PEH [8]. When the MPP has reached, the MPPT controller will enable the buck converter to transfer the energy from C_i and the PEH to C_S. Therefore, the duty cycle of the buck converter is not changed and the buck converter is able to provide a well regulated output voltage which can be used to safely charge up the supercapacitor. After the energy transfer from the input of buck converter to its output, voltage at C_i will drop while voltage V_S across C_S will increase. The buck converter will be disabled and there will be no energy transfer until the next MPP is reached. With both the buck converter and EAI disabled, there is no discharge path for C_S to ensure that energy can be accumulated for use by the WSN. This process repeats until V_S reaches the threshold voltage of EAI for energy release. The MPPT process is still ongoing when C_S discharges.

TABLE I. COMPONENTS AND CIRCUIT PARAMETERS

Component	Part Number	Circuit Parameters
Schottky Diodes	BAS70	V_F = 0.41 V@1 mA
Buck Converter	LTC3388-3	2.7 – 20 V_{in}; 3.3 V_{out}
C_i	TRJD226K035R0400	22 µF; ESR = 0.4mΩ
C_S	BZ054B223ZSBBQ	22 mF; ESR = 0.204mΩ

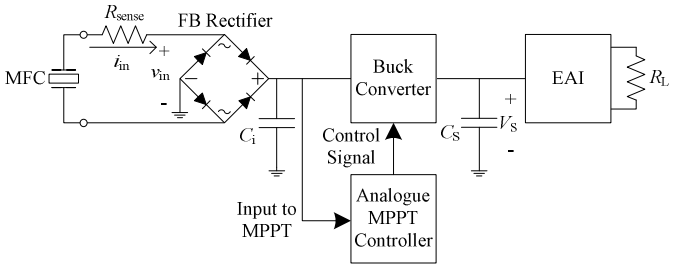

Fig. 3. Experimental setup for the proposed power management circuit.

C. Test Setup

Fig. 3 depicts the experiment setup to evaluate the performance of the proposed circuit which is implemented on a breadboard. A M8528-P2 macro-fiber composite (MFC) from Smart Material GmbH–Dresden, Germany bonded on a composite material is used as the PEH. Electrodes of the MFC PEH were connected to the prototyped circuit. This MFC-composite test specimen was excited by an Instron dynamic and fatigue test machine at frequency of 10 Hz with peak-to-peak strain level across the specimen measured at 364.82 με. Further tests with the same strain level were also conducted at vibrational frequencies of 20, 30, 40, 60, 70, 80, 90, and 100 Hz to verify the performance of the circuit at different frequencies. To evaluate the adaptability of the circuit to variations of the input voltage amplitude, the experiment was repeated at peak-to-peak strain level of 486.42 με and 972.85με at frequencies of 10, 20, 30 and 40 Hz. Test at 50 Hz was avoided as the Instron machine will resonate at that frequency. The machine would take longer time to reach steady state at high frequency, high loading test. Since the interest is to determine the adaptability of the proposed circuit to changes in amplitude in the second test with higher strain levels, the frequency were limited to 40 Hz.

Voltage and current from the MFC connected to the proposed circuit were measured and recorded using data acquisition (DAQ) system from National Instruments. The current was obtained by measuring the potential drop across a small 20 Ω resistor R_{sense}. Input power to the power management circuit can then be obtained by multiplying the root mean square of the measured input current and input voltage. The buck converter was set to provide constant voltage of 3.3 V. A 500 Ω resistive load R_L is used to simulate a WSN drawing an average of 5 mA from C_S. This current consumption is a good approximation for WSN using 802.15.4/ZigBee protocol [9]. The EAI was set to allow C_S to discharge to the load at 3.3 V until the V_S drops to 2.0 V because many WSNs can operate in the voltage range of 1.8 V to 3.6 V [9]. C_S used in this experiment is a 22 mF supercapacitor because with this capacitance value, it would take a few seconds to discharge from 3.3 V to 2.0 V through R_L, providing a reasonable window for a WSN to complete certain tasks. V_S was measured to record the charge and discharge cycles of C_S. The input power obtained using the proposed circuit was compared to the power harvested from the same MFC connected to optimal resistive load at the given test condition so that the overall efficiency of the circuit including the MPPT capability can be obtained.

III. EXPERIMENTAL RESULTS

Fig. 4a shows the input voltage v_{in} and voltage V_S across C_S at 100 Hz. Similar results were observed for other test conditions. It can be seen that the input voltage is not affected when C_S is discharging. The circuit is able to transfer the energy at the MPP for a given test condition regardless of the loading. A scaled image with $v_{in}/4$ and V_S is given in Fig. 4b showing that the voltage waveform during charging phase and discharging phase as separated by a solid vertical line is the same. This shows the stability and adaptability of the whole system in terms of performing the MPPT and transferring the energy from the MFC to the load.

Performance of the proposed circuit towards variation in vibrational frequency is verified from the measuremental results as shown in Fig. 5. Output power of the MFC is a function which increases with the square of vibration frequency as given by (1) [10]:

$$P = \frac{1}{2} V_{OC}^2 \frac{R_L}{\left(R_{MFC} + R_L\right)^2 + \left(1/\left(\omega C_{MFC}\right)\right)^2} \qquad (1)$$

where V_{OC} is the open-circuit voltage from the MFC, R_{MFC} and C_{MFC} are the equivalent resistance and capacitance of the MFC respectively. By using (1) and parameters shown in Table II, a power against frequency graph is plotted in Fig. 5 as well to see the trend of power generated by the MFC. Values of V_{OC}, R_{MFC} and C_{MFC} used in (1) were obtained via experimental measurements as shown in Table II. R_L was set to be equal to R_{MFC}, simulating a matched resistive load condition. The closely matched results from both experiment and equation proved that the power extraction capability of the circuit is independent of the load resistance as a fixed 500 Ω load is used throughout the experiment. The circuit is shown to be able to adapt to changes in vibration frequency and amplitude as well. Power harvested is low at low strain level and low frequency. It gradually became higher with increasing strain levels and vibrational frequencies. The trends of harvested power are the same for all the tests, justifying the adaptability and stability of the circuit over a wide vibrational spectrum.

The overall efficiency of the prototyped circuit is given in Fig. 6. At low strain level of 364.82 με, especially from 10 to 30 Hz, the efficiency is between 55% and 58%. The efficiencies for the rest of the tests are around 63 to 68%. The reason for the low efficiency at lower strain level is because with less input energy, the output energy from the buck converter will be low as well. From the data sheet, it can be seen that the efficiency of the buck converter suffers when the output current is low. The efficiency also becomes lower with higher input voltages, which explained the decreasing efficiency for the test at 972.85 με as the voltage is increasing with frequency. Due to the differences in the features and test conditions, it is not possible to make a direct comparison with other energy harvesting circuits. However, a summary of several state-of-the-art power management circuits using only one DC–DC converter is given in Table III to evaluate the performance of the proposed circuit.

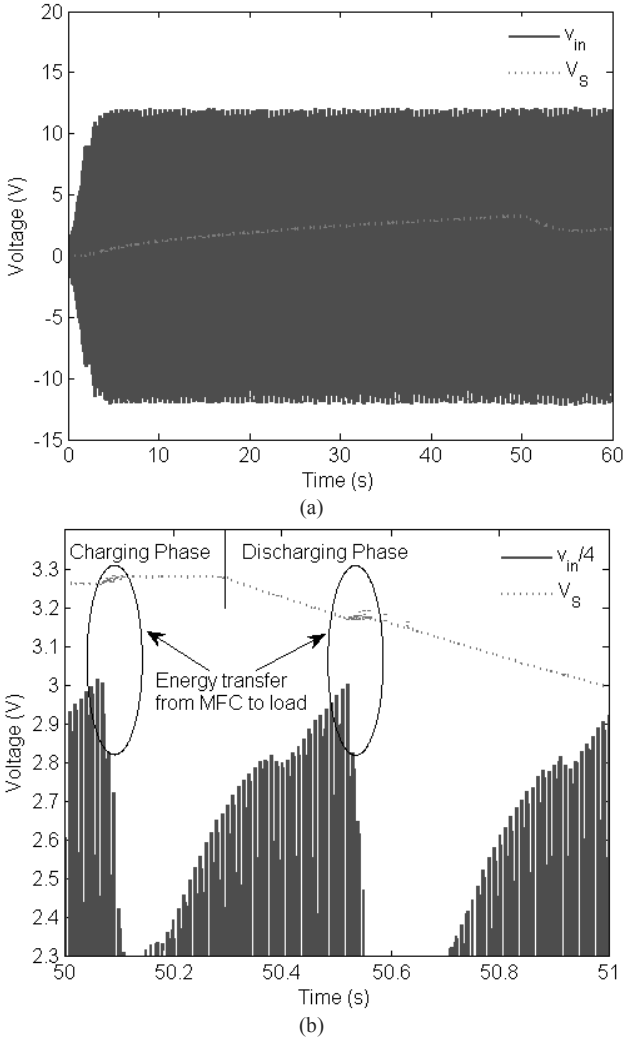

Fig. 4. Measured input voltage and voltage V_S across the storage capacitor C_S at 100 Hz showing the stability of the proposed circuit at: (a) full scale and (b) large scale at time period between 50 to 51s.

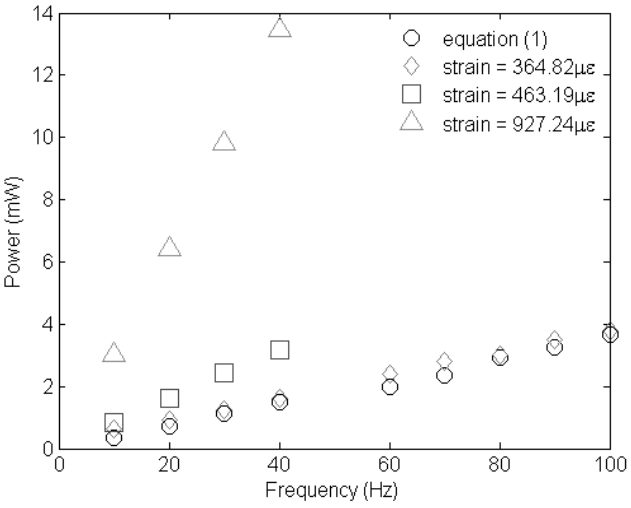

Fig. 5. Adaptability of the proposed circuit towards frequency changes.

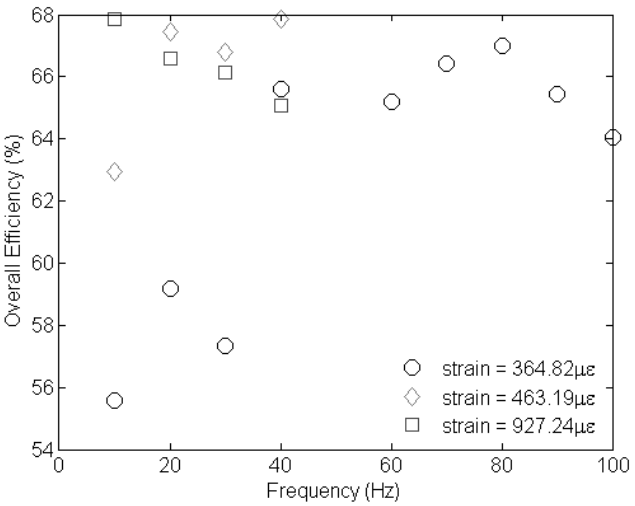

Fig. 6. Overall efficiencies of the proposed circuit under different test conditions.

TABLE II. PARAMETERS USED IN EQUATION (1)

Frequency (Hz)	Parameters		
	V_{OC} (Vpeak)	R_{MFC} (Ω)	C_{MFC} (nF)
10	18.98	8078	158.24
20	19.11	1362	159.79
30	19.36	1261	159.34
40	19.37	925	157.29
60	18.39	867	157.20
70	18.40	716	157.09
80	19.28	655	156.08
90	19.29	614	155.33
100	19.30	484	156.98

TABLE III. COMPARISON OF THE STATE-OF-THE-ART POWER MANAGEMENT CIRCUIT FOR PIEZOELECTRIC ENERGY HARVESTING WITH MPPT AND ONE DC–DC CONVERTER

Ref.	Parameters			
	Energy Storage	*MPPT Controller*	*Test Conditions*	*Efficiency*
[11]	Battery	Analogue	Function generator with capacitor as PEH; V_{OC} = 7.5 V±20%; 250 Hz ±20%	60%
[12]	Supercap	Microcontroller	PZT Cantilever; 44 to 53 Hz with resonant at 47 Hz; Optimal load from 10 to 50 kΩ	62–72%
This work	Supercap	Analogue	MFC PEH; 10 to 100 Hz at strains 364.82με, 463.19με, and 972.85με; R_L 500 Ω	normally 62–68%; 55–58% at low input energy;

IV. CONCLUSION

A low power adaptive circuit for harvesting energy from a PEH was presented. Performance the circuit is stable over a wide range of frequency and different loading conditions. Efficiency of the circuit is around 66% for most of the time except for low input energy conditions, indicating the efficiency of the DC–DC converter has a big influence on the overall efficiency of the system. This also clarifies the advantage of using only one DC–DC converter over two DC–DC converters to maintain higher overall efficiency of the system. A high efficiency DC–DC converter should be used to improve the performance of the power management circuit. Incorporating an EAI in the circuit is a viable solution to replace the regulating DC–DC converter without compromising the performance of the whole circuit.

ACKNOWLEDGMENT

The authors gratefully acknowledge financial support from the Technology Strategy Board (TSB)/Innovate UK via the project entitled “SENTIENT” (TSB 29640-211185) and EPSRC via the project entitled “SMARTER” (EP/K017950/1).

REFERENCES

[1] R. A. Steven and A. S. Henry, "A review of power harvesting using piezoelectric materials (2003–2006)," *Smart Materials and Structures,* vol. 16, pp. R1 - R21, 2007.

[2] S. Roundy, P. K. Wright, and J. Rabaey, "A study of low level vibrations as a power source for wireless sensor nodes," *Computer Communications,* vol. 26, pp. 1131-1144, July 1 2003.

[3] M. Zhu, E. Worthington, and J. Njuguna, "Analyses of power output of piezoelectric energy-harvesting devices directly connected to a load resistor using a coupled piezoelectric-circuit finite element method," *IEEE Transactions on Ultrasonics, Ferroelectrics and Frequency Control,* vol. 56, pp. 1309-1317, 2009.

[4] A. Ramond, G. A. A. Rodríguez, H. Durou, B. Jammes, and C. Rossi, "A SIDO buck converter with ultra low power MPPT scheme for optimized vibrational energy harvesting and management," in *Proceedings Power MEMS*, Washington DC, USA, 2009, pp. 415-418.

[5] X.-D. Do, S.-K. Han, and S.-G. Lee, "Optimization of piezoelectric energy harvesting systems by using a MPPT method," in *IEEE Fifth International Conference on Communications and Electronics (ICCE)*, 2014, pp. 309-312.

[6] Linear Technology, "LTC3388 - 20V High Efficiency Nanopower Step-Down Regulator," LTC3388-3 datasheet, 2010. Available: http://www.linear.com/product/LTC3388

[7] V. Marsic, M. Zhu, and S. Williams, "Wireless Sensor Communication System with Low Power Consumption for Integration with Energy Harvesting Technology," *Telfor Journal,* vol. 4, pp. 89-94, 2012.

[8] Z. J. Chew and M. Zhu, "Microwatt power consumption maximum power point tracking circuit using an analogue differentiator for piezoelectric energy harvesting," unpublished.

[9] E. Casilari, J. M. Cano-García, and G. Campos-Garrido, "Modeling of Current Consumption in 802.15.4/ZigBee Sensor Motes," *Sensors,* vol. 10, pp. 5443-5468, 2010.

[10] M. Pozzi, A. Canziani, I. Durazo-Cardenas, and M. Zhu, "Experimental characterisation of macro fibre composites and monolithic piezoelectric transducers for strain energy harvesting," 2012, pp. 834832-1/10.

[11] A. Tabesh and L. G. Fréchette, "A Low-Power Stand-Alone Adaptive Circuit for Harvesting Energy From a Piezoelectric Micropower Generator," *IEEE Transactions on Industrial Electronics,* vol. 57, pp. 840-849, 2010.

[12] N. Kong and D.-S. Ha, "Low-Power Design of a Self-powered Piezoelectric Energy Harvesting System With Maximum Power Point Tracking," *IEEE Transactions on Power Electronics,* vol. 27, pp. 2298-2308, 2012.